

BILINEAR MODELING AND NONLINEAR ESTIMATION *

Thomas A.W.Dwyer III Fakhreddine Karray
Department of Aeronautical and Astronautical Engineering
University of Illinois ,Urbana,IL 61801
and
William H. Bennett
Techno-Sciences,Inc. 7833 Walker Drive,Greenbelt,MD 20770

Abstract: In This paper we illustrate new methods of online nonlinear estimation applied to the lateral deflection of an elastic beam from on board measurements of angular rates and angular accelerations. We contrast the development of the filter equations, together with practical issues of their numerical solution as developed from global linearization by nonlinear output injection with the usual method of the the extended Kalman filter(EKF). We show how nonlinear estimation due to gyroscopic coupling can be implemented as an adptive covariance filter using off-the-shelf Kalman filter alghorithms. The effect of the global linearization by nonlinear output injection is to introduce a change of coordinates in which only the process noise covariance is to be updated in online implementation. This is in contrast to the computational approach which arises in EKF methods arising by local linearization with respect to the current conditional mean. We also highlight processing refinements for nonlinear estimation based on optimal ,nonlinear interpolation between observations. In these methods the extrapolation of the process dynamics between measurement updates is obtained by replacing a transition matrix with an operator spline that is optimized off-line from responses to selected test inputs .

*Supported in part by SDIO/IST and managed by AFSOR under contract F49620-87-C-0103, and by NASA grant NAG-1-613

1 Introduction

In this paper, a new nonlinear, nonparametric method is proposed for off-line modeling and on-line estimation of nonlinear dynamic systems. For illustration, it is applied to the estimation of the deformation of an elastic structure, undergoing rapid rotational maneuvers.

In these circumstances, the structural stiffness and damping coefficients depend on the angular acceleration $\dot{\omega}$, the angular rate ω and the square of the angular rate. In the single axis case, the excitation of the structure is represented by the vector $u^T = (\dot{\omega}, \omega^2, 2\omega)$, to which the structural dynamics responds as a "bilinear" (i.e., parametrically excited) system. A similar technique for multiaxial rotations yields a bilinear model with respect to matrix valued excitations.

Two methods of estimation and modeling are combined to achieve deformation state determination:

- A method based on a feedback linearized procedure which gives an estimate by a filter constructed from the equivalent linear dynamics, which is faster than the extended Kalman filter.
- The modeling of the deformation state of the structure by means of a Volterra series interpolator.

2 Simplified Model of a Deformable Structure and Equations of Motion

For purposes of illustration of the principles involved, the structure will consist of a primary mirror, attached to a spacecraft (containing the hardware of the slewing controller), and a secondary mirror attached to the central one in the shape of a Cassegrain telescope by means of massless links. The primary mirror structure will also be regarded as attached to the spacecraft by means of a massless link. Equivalently the same model can be thought to represent a laser beam expander, as in Figure 1. More realistic models, such as in [1] or [2], exhibit the same form of interaction between the rotational and vibrational dynamics. The simplified telescope part of the structure can itself be modeled as a system of two masses attached together by a single "equivalent" link, with "equivalent" stiffness and damping coefficients, so that the same restoring and dissipation forces at the secondary are obtained as if with more than one link. The modeling of such a deformable body is

summarized in Figure 2 .

If one takes now only the vibrational equation of motion ,and set the rotation around a single axis \vec{b}^3 ,i.e, $\vec{\omega} = \dot{\theta}\vec{b}^3$,and if the translational acceleration term is substituted from the translational equation, then one finds:

$$M\ddot{\mathbf{y}} + (C + 2\dot{\theta}\bar{J}M)\dot{\mathbf{y}} + (K + (\ddot{\theta} + \bar{J}\dot{\theta}^2)\bar{J}M)\mathbf{y} + (\ddot{\theta} + \dot{\theta}^2\bar{J})\bar{J}M\rho = \mathbf{f} \quad (1)$$

where \bar{J} is not an inertia term, but rather an augmented symplectic matrix, made of blocks $\begin{pmatrix} 0 & -1 \\ 1 & 0 \end{pmatrix}$ while M is a modified structure mass matrix to account for contributions due to translation, and ρ is the $2n \times 1$ matrix components of the vectors ρ_i from the undeformed appendage mass centers. Here \mathbf{y} denotes the $(2n \times 1)$ (for planar motion or $(3n \times 1)$ for out of plane motion) matrix of deflection coordinates of the center of mass of n appendages from their undeformed positions, $n = 2$ in the case of the secondary mirror and the spacecraft platform regarded as appendages of the primary.

\mathbf{f} is the $(2n \times 1)$ (say, 4×1 here) matrix of body coordinates of external forces acting on the centers of mass of the n appendages.

All other notations used are found in [12],[13].

Let now η be a new variable such that

$$\eta = M(\mathbf{y} + \rho) \quad (2)$$

and let

$$\tilde{C} = CM^{-1} \quad (3)$$

$$\tilde{K} = KM^{-1} \quad (4)$$

as well as

$$\mathbf{u}^T = (\dot{\omega}, \omega^2, 2\omega) \quad (5)$$

Then the vibrational equation of motion becomes:

$$\ddot{\eta} + (\tilde{C} + u_3\bar{J})\dot{\eta} + (\tilde{K} + u_1\bar{J} + u_3\bar{J}^2)\eta = \mathbf{f} + K\rho \quad (6)$$

This transformed equation can also be written in the bilinear form ,which will be used frequently in the following sections,

$$\dot{\mathbf{X}} = A\mathbf{X} + B(\mathbf{X})\mathbf{u} + \mathbf{b} \quad (7)$$

where:

$$A = \begin{pmatrix} [0] & [I] \\ [-\tilde{K}] & [-\tilde{C}] \end{pmatrix} \quad (8)$$

$$B(\mathbf{X}) = \begin{pmatrix} [0] & [0] & [0] \\ \bar{J}\mathbf{X}_1 & \bar{J}^2\mathbf{X}_1 & \bar{J}\mathbf{X}_2 \end{pmatrix} \quad (9)$$

and

$$\mathbf{b} = \begin{pmatrix} [0] \\ \mathbf{f} + K\rho \end{pmatrix} \quad (10)$$

while \mathbf{X}_1 and \mathbf{X}_2 are the vector components of the state vector $\mathbf{X} = (\eta^T, \dot{\eta}^T)^T$.

This simplified model, insofar as the links are regarded to be mass-less, exhibits all the coupling effects between slewing motion and vibrational motion. A distributed model under the assumption of symmetry about the mass center also yields product terms between $\dot{\theta}^2$ and structural deformations, and can be found in Chapter 9 of the book by Junkins and Turner[3]. That model of a symmetric four appendage spacecraft can also be used to illustrate the procedures being developed in this study, if desired, although damping must be present, so that the matrix A above will be stable. A slewing Timoshenko beam model likewise exhibits this gyroscopic coupling effect, and also accounts for damping, so that A becomes stable, as found in [4].

3 Estimation of the state by means of observers

This part of the estimation technique will deal mainly with updating the state from sensor data.

3.1 Extended Kalman filter formulation

Usually, when one deals with a nonlinear system of which the state variables cannot all be observed (or are corrupted with noise), then the most commonly used method of filtering or smoothing is the extended Kalman filter formulation [5]. Let the dynamical system be modeled as shown,

$$\begin{cases} \dot{x} = f(x) + G(x)u^* + G(x)\xi \\ y = h(x + \nu) \end{cases} \quad (11)$$

where u^* is the deterministic (mean) part of the input, ξ is a zero mean input noise, and h is defined in our case as $h = (h_1^T, h_2^T)^T$, where

$$\begin{cases} h_1(.) = M^{-1}(. - \mathbf{n}) \\ h_2(.) = M^{-1}(.) \end{cases} \quad (12)$$

Let $R_i\delta(t - \tau) = E[\nu_i(t)\nu_i(\tau)^T]$ be the covariance matrix of the sensor noise vectors ν_i , with $R = \text{diag}(R_1, R_2)$ and let $Q\delta(t - \tau) = E[\xi(t)\xi(\tau)^T]$ be

the covariance matrix of the actuator noise with ν_i and ξ presumed to be uncorrelated for simplicity.

The propagation error matrix is defined by P , which satisfies the following Riccati differential equation along the estimated state trajectory \hat{x} :

$$\begin{aligned} \dot{P} = & \left[\frac{\partial f}{\partial x} \right]_{\hat{x}} P + P \left[\frac{\partial f}{\partial x} \right]_{\hat{x}}^T + G(\hat{x}) Q G(\hat{x})^T - \\ & P \left[\frac{\partial h}{\partial x} \right]_{\hat{x}}^T R^{-1} \left[\frac{\partial h}{\partial x} \right]_{\hat{x}} P \end{aligned} \quad (13)$$

\hat{x} can be expressed as an observer,

$$\begin{cases} \dot{\hat{x}} = f(\hat{x}) + G(\hat{x})u^* + K(y - \hat{y}) \\ \hat{y} = h(\hat{x}) \end{cases} \quad (14)$$

where K is the extended Kalman gain, and is defined as follows:

$$K = P \left[\frac{\partial h}{\partial x} \right]_{\hat{x}}^T R^{-1} \quad (15)$$

A procedure [6] based on a change of variables, in preliminary studies gave a faster computation time. This procedure is outlined next.

3.2 Feedback linearized procedure:

The idea is to change the state configuration of the original system, which has the particular form below:

$$\begin{cases} \dot{x}_1 = F_1(x_1)x_2 \\ \dot{x}_2 = F_2(x)(u^* + \xi) + f_2(x) \end{cases} \quad (16)$$

$$\begin{cases} y_1 = h_1(x_1 + \nu_1) \\ y_2 = h_2(x_2 + \nu_2) \end{cases} \quad (17)$$

By using the change of variables $x'_1 = x_1, x'_2 = F_1(x_1)x_2$, $u' = \ddot{x}_1 = F_2(x)u^* + f_2(x)$ and $y'_1 = h_1^{-1}(y_1), y'_2 = h_2^{-1}(y_2)$ one gets

$$\begin{cases} \dot{x}'_1 = x'_2 \\ \dot{x}'_2 = u'^* + \xi' \end{cases} \quad (18)$$

where $\xi' = F_1 F_2 \xi$ and $\nu'_i = F_1 \nu_i$, so that the covariance of ξ' is approximated by

$$Q' = F_1(\hat{x}_1) F_2(\hat{x}) Q F_2(\hat{x})^T F_1(\hat{x}_1)^T \quad (19)$$

while that for ν'_i is approximated by

$$R'_i = F_1(\hat{x}_1) R_i F_1(\hat{x}_1)^T \quad (20)$$

Then the new error covariance matrix propagation is derived from the following Riccati differential equation:

$$\begin{aligned} \dot{P}' = & \begin{pmatrix} [0] & [I] \\ [0] & [0] \end{pmatrix} P' + P' \begin{pmatrix} [0] & [0] \\ [I] & [0] \end{pmatrix} + \\ & \begin{pmatrix} [0] \\ [I] \end{pmatrix} Q' \begin{pmatrix} [0] & [I] \end{pmatrix} - \\ & P' \begin{pmatrix} [I] & [0] \\ [0] & [I] \end{pmatrix} R'^{-1} \begin{pmatrix} [I] & [0] \\ [0] & [I] \end{pmatrix} P' \end{aligned} \quad (21)$$

The observed deformation state is also propagated in the usual manner:

$$\begin{aligned} \dot{\hat{x}}'(t) = & \left\{ \begin{pmatrix} [0] & [I] \\ [0] & [0] \end{pmatrix} - K' \begin{pmatrix} [I] & [0] \\ [0] & [I] \end{pmatrix} \right\} \hat{x}'(t) + \\ & \begin{pmatrix} [0] \\ [I] \end{pmatrix} u' + P'(t, t_0) R'(t)^{-1} \begin{pmatrix} h_1^{-1}(\cdot) & [0] \\ [0] & F_1 h_2^{-1}(\cdot) \end{pmatrix} y(t) \end{aligned} \quad (22)$$

where the innovation process gain is now given as follows:

$$K' = P'(t, t_0) R'(t)^{-1} \quad (23)$$

For the case of single axis slew-induced structural deformation estimation one has $F_1 = I$ and $F_2 =$ lower half of $B(X)$ defined by equation (2). In particular, one finds $R'_i = R_i$, so that, in contrast to the extended Kalman filter, only the P' -independent forcing term of the equation (21) given by Q' has to be updated, all coefficients being now constants. In dealing with this procedure a 25% increase in speed, with comparable accuracy has been found in preliminary simulations discussed below. The problem in using either one of those two estimation techniques (even the faster one) in more realistic models than the example used here, is the high dimensionality of the filter then required, which may not be accommodated by the on-board data processing rate, causing estimation delays.

C-4

3.3 Estimation Examples:

A simplified model of a beam expander was represented by a primary mirror mass elastically linked to a secondary mirror mass according to the simplified model outlined in Section 2. Restoring forces and dissipative forces proportional to relative secondary mirror motion were modeled at the secondary. The structural parameters are found in the companion example in Subsection 5.1. A piecewise constant angular acceleration was commanded, representing the acceleration-deceleration profile of a minimum time retargeting maneuver. The commanded angular acceleration profile was:

$$\dot{\omega}(t) = \begin{cases} 0.3 \text{ rad.s}^{-2} & \text{if } 0 \leq t \leq .5(s); \\ -0.3 \text{ rad.s}^{-2} & \text{if } .5(s) \leq t \leq 1(s); \end{cases}$$

Presumed angular accelerometer and gyro noise covariances were transformed into equivalent process noise for the feedback-linearized filter, with the additional simplification of neglecting a square noise term corresponding to the second entry $u_2 = \omega^2$ of the equivalent input u . Presumed strain gauge sensor noises were taken from the literature. The sensor noise covariance matrix was modeled as a diagonal matrix with all diagonal elements equal to 0.00018. Likewise the input covariance for u_1 was 0.000005 and for u_3 was 0.00001. The input covariance related to the input u_2 was supposed to be negligible with respect to the other two. Two simulations were made, each one of them to illustrate the two methods of estimation described above. The first simulation was made without active bias suppression, i.e. $\mathbf{f} = \mathbf{0}$ in equation (10), the results being shown in Figures 3, 4. The second simulation was made with the use of bias suppression making $\mathbf{b} = \mathbf{0}$ in equation (7) by letting $\mathbf{f} = -\mathbf{K}\rho$, the results being shown in Figures 5, 6.

4 Off Line Modeling

In this section the method of Optimal Bilinear System Interpolation is used. In this technique the dynamical system is represented in bilinear form (by active suppression, if needed, of the bias term \mathbf{b}),

$$\begin{cases} \dot{\mathbf{X}} &= \mathbf{A}\mathbf{X} + \mathbf{B}(\mathbf{X})\mathbf{u} \\ \mathbf{y} &= \mathbf{c}^T \mathbf{X} \end{cases} \quad (24)$$

where $\mathbf{B}(\mathbf{X}) = [\mathbf{B}_1\mathbf{X} \mid \mathbf{B}_2\mathbf{X} \mid \dots]$. This also means:

- The (I/ O) behavior is highly nonlinear.
- The model is high dimensional if arising from Carleman linearization.
- There is no clean ARMA model for system identification.

Then, by using optimal interpolation one finds:

- A closed form, circuit-implementable, reduced order, decoupled model which is also bilinear: cf. Figure 7.
- (I/ O)-based system identification can be used to tune the model to known responses to designer-selected typical excitations.
- The dimension of the new system model is equal to the number of test signals.

In the present application, the model is "a priori" bilinear by the choice made for the inputs, so that the dimension is that of the structural model, here given by the number of mass points. For more realistic structural models, the filter dimension would nevertheless be high. Rather than tolerate the time delay found in the previous techniques of estimation, the method of operator spline interpolation can be used, to find the deflection amount between observations. The input-output (I/O) operator V ,

$$V : u \rightarrow y \quad (25)$$

from the excitation vector u to an output vector y (such as ν given by equation (2)) is imbedded in a Hilbert space of (I/O) operators of candidate bilinear systems, equipped with a reproducing kernel, see equation (31)

$$K_t(u, v) = \exp \int_{t_0}^t u^T(s) R^{-1} v(s) ds \quad (26)$$

where the weight matrix R is determined by eigenvalues of A in equation (24), which in the context of the present application corresponds to bounds on the structural frequencies. An interpolator of the form

$$\hat{V}_t(u) = \sum_i c_i(t) K_t(u, u^i) \quad (27)$$

is constructed, tuned so that the structural responses to preselected test inputs u^i are recorded, and optimally interpolating at system level the responses to other excitations in the signal class.

If the recorded system responses y^i to the test input u^i are reliably known, the 'tuned' coefficients c_i are obtained by solving the matrix equation

$$G(t)c(t) = \bar{y}(t) \quad (28)$$

where $c(t) = \text{col}\{c_i\}$, $\bar{y}(t) = \text{col}\{y^i(t)\}$ and $G(t) = \{K_t(u^i, u^j)\}_{i,j}$. A more complex matrix equation yields the c_i for uncertain y^i : cf. [7], [8], [9]. The optimization leading to the functional interpolator \hat{V}_t is formulated as a minimization of the maximum distance between the interpolating operator and any candidate operator that matches the experimental input-output signals. If the system data are not accurate, a weighted minimization that does not require exact matching of system responses can also be used. This minimization is carried out in a Hilbert space of input-output operators equipped with a weighted "Fock space" scalar product which is the Hilbert sum of the causal (i.e., with lower triangular domains of integration) L^2 scalar products of the kernels of the Volterra series of the operators in question, for which K_t is the reproducing kernel. The general method is discussed in [9], although causality was differently implemented there, since symmetric kernels were used.

The Hilbert space structure for m inputs (here $m = 3$) is defined as follows: let

$$\begin{aligned} h_{n,i_1,\dots,i_n}(t, t_1, \dots, t_n) &= c^T \exp\{(t - t_1)A\} B_{i_1} \dots \\ &\dots \exp\{(t_{n-1} - t_n)A\} B_{i_n} \exp(t_n A) X(0) \end{aligned} \quad (29)$$

where $B(X) = [B_1(X) \mid B_2(X) \mid \dots]$ and $i_1, \dots, i_n \in \{1, \dots, m\}$.

These are the Volterra kernels for $u_{i_1}(t_1), \dots, u_{i_n}(t_n)$ so long as triangular integration is used as in equation (30). Then the inner product is given as shown ,

$$\langle V_t, V_t \rangle = \sum_n \sum_{i_1} \dots \sum_{i_n} r_{i_1} \dots r_{i_n} \int_0^t \int_0^{t_1} \dots$$

$$\int_0^{t_n} h_{n,i_1,\dots,i_n}(t, t_1, \dots, t_n) h_{n,i_1,\dots,i_n}(t, t_1, \dots, t_n) dt_n \dots dt_1 \quad (30)$$

with designer-selected weights $r_i > 0$ corresponding to $R = \text{diag}\{r_i\}$, which yields the reproducing property:

$$\langle V_t, K_t(u, \cdot) \rangle = V_t(u) \quad (31)$$

The Volterra series for a bilinear system will yield a bounded norm $\langle V_t, V_t \rangle$ provided the weights r_j are chosen so that

$$\sum_i r_i \|B_i\|^2 \leq \frac{2a}{N} \quad (32)$$

where $N = \dim X$ and " a " is a bound on the real parts of the eigenvalues of A , so that $\| \exp(At) \|^2 \leq N \exp(-2at)$. The bound (32) is obtained after cancellation of intermediate exponents in the factors $\exp\{-2a(t_{i-1} - t_i)\}$, which can be interchanged when computing L^2 bounds of $|h_{n,i_1,\dots,i_n}(t, t_1, \dots, t_n)|$, to guarantee negativity of the remaining exponential coefficients. The same bound is sufficient for having $|\hat{y}(t)| = |\hat{V}_t(u)| \rightarrow 0$ as $t \rightarrow \infty$ when u is L^2 (Square integrable), as is found by use of the reproducing property (31) (Lower bounds are also needed when the inputs are not L^2 , but are bounded almost everywhere: Dwyer, [7]). The advantages of such modeling are:

- The model dimension is equal to the number of test inputs.
- The modeling error is distributed throughout the chosen input signal class (i.e. by frequency or amplitude), rather than depending on nearness to a single reference input.
- The interpolated signal(response) can be proven to converge asymptotically to the true system response for any (unknown) excitation in the chosen signal class.

In this technique of modeling, the real data $\eta^{(i)}$, $\dot{\eta}^{(i)}$ can be recorded by exciting the real system with (constant or nonconstant) test inputs to construct the interpolator. The test inputs can be chosen to approximate the expected excitations of the system. Thus, the real system time responses are used for model matching, rather than responses synthesized from the mathematical

model.

The problem with this technique, however, lies in the fact that storage of curves is required in order to compute the c_i 's. The number of stored curves is equal to $m \times k \times I^N$, where m is the number of test inputs, k is the dimension of the output vector y , N the dimension of the state to be modeled and I is the number of possible initial values of each component. This difficulty does not allow the system to run in real time: e.g., for the case of n point masses linked by massless but elastic connections one has $N = 2n$ and $k = n$ when measuring deflections or $k = N = 2n$ if full state information is required in the planar motion case.

5 Interpolator-Based Estimation:

In this section, the two last techniques are combined to create a more effective one by making use of the transition matrix spline of the bilinear system of the model:

$$\hat{\eta}(t) = \hat{\Phi}(t, t_k) \hat{\eta}(t, t_k) \quad (33)$$

In fact, the matrix-valued operator spline $\hat{\Phi}$ interpolates the transition matrices Φ_i corresponding to the bilinear system model excited by constant or piecewise constant test inputs $u^{(i)}$. This permits the construction of the response of the real time system in piecewise closed form, thereby replacing response curve storage by an analytic transition matrix generator, rather than the construction of the coefficients interpolator c_i from the output test signals $y^T = (y^1, y^2, \dots, y^m)$.

One gets each entry c_i^{pq} of the matrix valued spline coefficients c_i by letting $\bar{y}^i = \Phi_i^{pq}$ in equation (28) where Φ_i^{pq} is the (p, q) -entry in the transition matrix with constant $u^{(i)}$:

$$\Phi_i = \exp\left\{(A + \sum_j B_j u_j^{(i)})t\right\} \quad (34)$$

The interpolated transition matrix is then used to update between observations the structural state estimates obtained from an adaptive covariance filter based on a globally feedback-linearized transformation (seen in Section 3.2) of the bilinear structural model.

This last technique has the following features:

- $\hat{\Phi}$ is open loop, with $\hat{\eta}$ made to match the real system at discrete

intervals by re-initializing:

$$\begin{pmatrix} \hat{\eta}(t) \\ \dot{\hat{\eta}}(t) \end{pmatrix} = \hat{\Phi}(t, t_k) \begin{pmatrix} \hat{\eta}(t_k) \\ \dot{\hat{\eta}}(t_k) \end{pmatrix} \quad (35)$$

In contrast, the direct modeling of the I/O operator

$$\hat{\eta} = \sum_i c_i(t) \exp \int^t u^T R^{-1} u^i dt \quad (36)$$

continuously tracks the true system time responses $\eta^i(t)$, but in this case $c_i(t)$ cannot be generated analytically and must be computed off-line.

- The presence of an additive input does not give rise to a steady state tracking error observed in the earlier literature when additive as well as multiplicative inputs are present, as is the case for rapidly slewing structures. Indeed, a convolution correction based on $\hat{\Phi}$ can be added, eliminating the need for active suppression of the bias term \mathbf{b} in equation (7).

- The number of curves to be generated is only $m \times N^2$ instead of $m \times k \times I^N$, (where again $N = 2n$ for the example of a structure composed of point masses connected by elastic appendages and in plane motion).

- The possibly high dimensional recursive filter can run at a slower sampling rate chosen to be consistent with on board CPU capabilities.

5.1 Interpolation Example

An interpolator was designed for the same two bodies beam expander model previously described: The interpolator was optimized for input vectors $u^T = (u_1, u_2, u_3)$ of the form $(constant, 0, 0)$, $(0, constant, 0)$ and $(0, 0, constant)$, chosen with a positive constant during the first half of a 1 second nominal minimum time rotation, and negative during the second half, for the first test input vector. The same positive constant was chosen throughout the 1 second repointing for the second and third test input vectors, this qualitatively correspond to the nominal angular motion where $\dot{\omega}$ is a square wave beginning at +0.3 and reversing, which yields positive (though not constant) values for ω_2 and 2ω : cf. Eq.(5). The constants were selected for boundedness of the interpolator according to [7],[8]. For the sake of convergence of the interpolator to the actual output of the system, and in the case of applying test inputs which are not square integrable, the matrix R described above in the reproducing kernel analytical form should have diagonal elements satisfying the following condition:

$$a/m - \sqrt{(a/m)^2 - \|B_i\|^2 N \lambda_i^2} \leq$$

$$r_i N \|B_i\|^2 \leq \frac{a/m + \sqrt{(a/m)^2 - \|B_i\|^2 N \lambda_i^2}}{2} \quad (37)$$

If A is $N \times N$, $\|B_i\|^2 = \sum_{pq} b_{i,pq}^2$ where $b_{i,pq}$ is the (p, q) element of B_i , then λ_i , which is the upper limit of the i -th test input component, must be chosen to satisfy the bounds below,

$$0 < \lambda_i < a/m\sqrt{N}\|B_i\| \quad (38)$$

where a is an upper bound on the real parts of the eigenvalues of the matrix A , and m is the number of test inputs applied to the interpolator. Indeed, the bound (41) allows selecting positive r_i 's in the inequality (37), which itself occurs in obtaining bounds on $\hat{y}(t) = V_t(u)$ from equation (34), to guarantee $\hat{y}(t) \rightarrow 0$:cf.[6]

In case the applied test inputs are square integrable, as will be chosen on the example, one needs only a simpler form of bounds for r_i described as follows, which implies the inequality (32) if all r_i are the same,

$$0 \leq r_i N \|B_i\|^2 \leq 2a/m \quad (39)$$

The data used to drive this example are very near to those of a space based laser model:

$$J_0 = 20,556 \text{ kg.m}^2, m^0 = 10,720 \text{ kg}, m^1 = 152 \text{ kg}, \rho^1 = (0, 14.421 \text{ m})^T$$

$$K = \begin{pmatrix} 1642 & 121.6 \\ 121.6 & 1355.8 \end{pmatrix}, \quad C = \begin{pmatrix} 162 & 120 \\ 120 & 1357 \end{pmatrix}$$

The nondiagonal form of the above matrices K and C is due to the fact that the two links that hold the small mirror in the top can be regarded as an equivalent link with equivalent stiffness and damping matrices, as shown in [13].

Now by applying those data to the system and by the choice of $constant = .3$ in the test inputs, one finds $0 \leq r_i \leq 1/12$ where $r_i = r$ for all i , giving $R = \text{diag}(r_i) = r[I]_{m \times m}$. Two series of simulations were made. In each one of them two alternatives, namely, bias elimination, i.e., $\mathbf{b} = \mathbf{0}$ or no external tip forces, i.e., $\mathbf{f} = \mathbf{0}$ are considered. In the first series of simulations the interpolator was used over the entire minimum time *1second* maneuver and thereafter. The results for the case of lateral deflection of the appendage are shown in Figures 8,9. It is important to notice here that in case of bias presence, a numerical convolution product was used with the original

transition matrix $\Phi(t, t_k)$ as well as with the interpolated transition matrix $\hat{\Phi}(t, t_k)$ for the sake of error comparisons. "Original" in the plots means the numerical solution of Eq.(1), "discrete" means the numerical computation of $\Phi_u(t, 0)x(0) + \Phi_u(t, \cdot) * b$. One last numerical difficulty was observed, in addition to care needed in generating the contribution from b by convolution (at least in this unusual beam expander example). That was the singularity of Eq.(28) at $t=0$ as already discussed in [9], which caused numerical unreliability during the first 0.25 seconds of this motion. Thus "transient error" is consistent with the "adaptive" nature of the interpolator which must "learn" from the system response to alleviate this numerical difficulty, in the other series the state estimated in the example of section 3.3 was used to re-initialize the interpolator each .5s. The results are shown in Figures 10,11. The re-initialization from the estimated state at given moments yielded better results than when using the same interpolator throughout.

6 Concluding Remarks

Filter algorithms combine the propagation of measurements "between" observations with updating of measurements "across" observations. Such updating to account for new observations has been shown here to be obtainable from an estimator based on a globally feedback-linearized model of a nonlinear process.

In case nonlinear transformation of the observed part of the process state is required, it was shown that the associated matrix Riccati differential equation for the propagation of the estimation error covariance needs to be updated only in its "driving" term, given by the process noise covariance. In contrast, all the coefficients of the Riccati equation for the corresponding extended Kalman filter must be updated, so that considerable CPU time is saved by pre-linearization, although the filter dimension is the same. Dimension reduction between measurements is therefore still desirable, motivating the next part of this work, which is reviewed below. If the process dynamics is "parametrically excited", e.g. by gyroscopic coupling, it was then shown how the process state can be propagated between observations by interpolation of the input-output operator that maps the process excitation to the (time-varying) state transition matrix. This interpolator was shown to be simultaneously optimized to match the measured system response to a set of pre-selected "test inputs", which if chosen piecewise constant can also be encoded analytically in closed form. Since the interpolator dimension is determined by the dimension of the pro-

cess state ,it is therefore faster to periodically re-start the interpolator at the rate the feedback linearized filter(or any other) can process full state information, rather than be tied down to the full order filter processing rate. New results were then given on the application of the method to the on-line estimation of transverse deflections of a rapidly slewing, gyroscopically slew-coupled beam expander,previously reported in [12]. Applications to line of sight disturbance error bound estimation in sliding control following [10] are also outlined in [11]. the interpolation technique may also be used to update observations for multi-axis motion of multibody systems , but this latter work is still undeveloped.

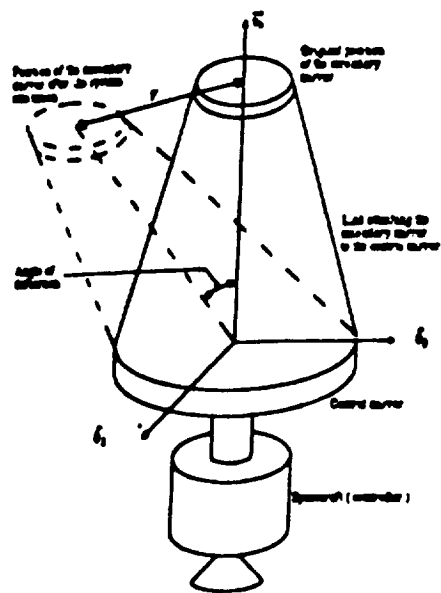
REFERENCES

1. T.R.Kane, R.R.Ryan and A.K.Banerjee,"Dynamics of a Cantilever Beam Attached to a Moving Base." *J. of Guidance, Control and Dynamics*,v.10,No.2(Mar-Apr. 1987),pp.139-151.
2. J. Baillieul,"Linearized Model For The Control Of Rotating Beams",*Proc IEEE CDC*, (Austin, Tx, Dec 7-9,1988),v.3,pp. 1726-1731.
3. J.L.Junkins and J.D.Turner, "Optimal Spacecraft Rotational Maneuvers" , Elsevier, 1986.
4. H.Bennett, H.G.Kwaty and G.L.Blankenship,"Nonlinear Dynamics and Control Issues for Space-Based Directed Energy Weapons",*Proc. 27th IEEE Conf on Decision and Control*,(Austin,Tx, Dec.7-9,1988).
5. A.Gelb,Ed ,"Applied Optimal Estimation", MIT Press,1974. break
6. M.S.Fadali, S.Gardner and T.A.W. Dwyer III , "Nonlinear Decoupling And Control Of Manipulators With Sensor And Actuator Noise.", *Proc. 2nd IASTED Internat Conf, on Applied Control and Identification* (Los An-

geles, CA, Dec.10 -12, 1986),Acta Press, Calgary, 1987.

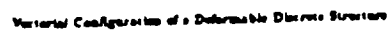
7. T.A.W. Dwyer III , "Operator Spline Methods in the Design of Non-linear Equalizers",*Proc.IEEE ISCAS* (San jose,CA,May 5-7,1986), v.2 ,pp. 701-703.
8. T.A.W. Dwyer III , "Optimal Interpolation and Smoothing Of Bilinear Systems",*Proc. ACC*(Seattle,WA, June 18-20, 1986), v. 1, pp 394-397.
9. R.J.P. de Figueiredo and T.A.W DwyerIII,"A Best Approximation Framework and Implementation for Simulation of Large-Scale Nonlinear Systems", *IEEE trans. on Circuits and Systems*,v.CAS-27, No.11 (Nov.1980), pp. 1005-1014.
10. J.J. E.Slotine, "Sliding Controller Design for Non-linear Systems", *int.J. of Control*,v.40, No.2(1984), pp.421-434.
11. T.A.W. Dwyer III and F. Karray,"Nonlinear Robust Variable Structure Control of Pointing and Tracking with Operator Spline Estimation",*Proc. IEEE International Symposium on Circuits and Systems*(Corvalis,Oregon, May 9-11,1989) Paper # SSP 15-5.
12. T.A.W. Dwyer III and F. Karray,"Nonlinear Modeling Identification and Estimation of Slew Induced Structural Deformations",*Proc. Model Determination for Large Space Systems Workshops*(Pasadena,CA, March22-24,1988) ,JPL D-5574,V3,pp860-876.
13. T.A.W. Dwyer III and F. Karray,"Bilinear Modeling and Estimation of Slew Induced Deformations", Submitted to *J. of Astronautical Sciences*.

ORIGINAL PAGE IS
OF POOR QUALITY



Simplified Design of The Open Laser Telescope Structure.

Figure 1.



ORIGINAL PAGE IS
OF POOR QUALITY

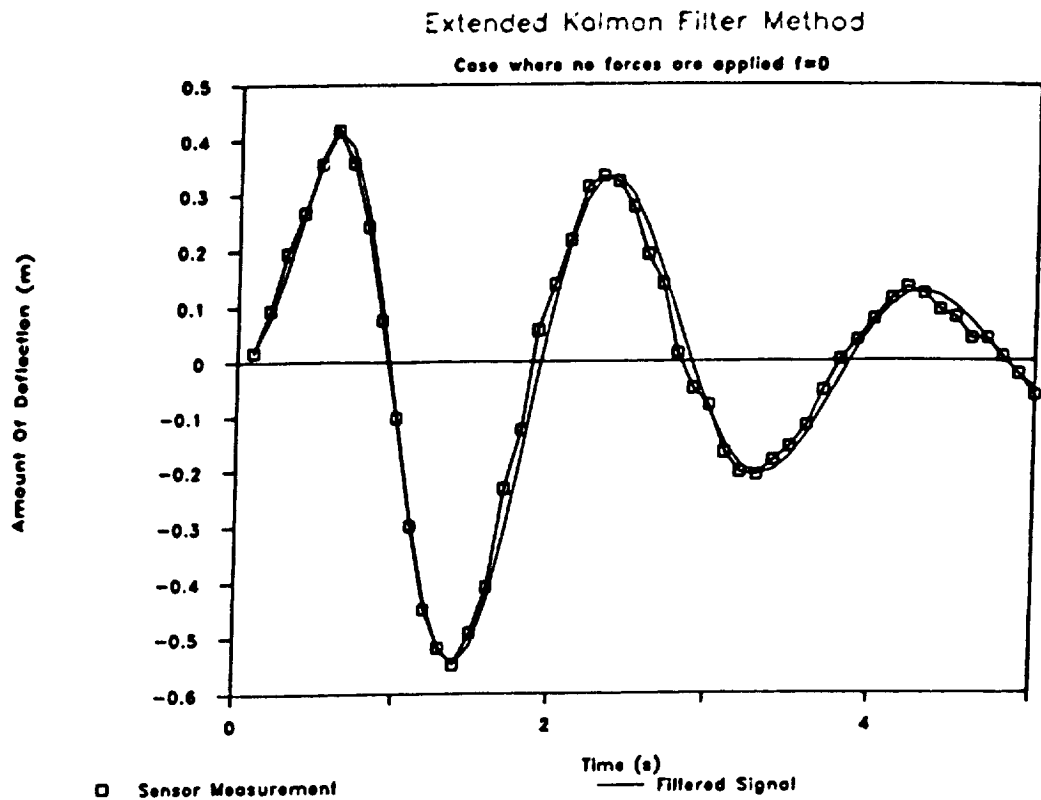


Figure 3.

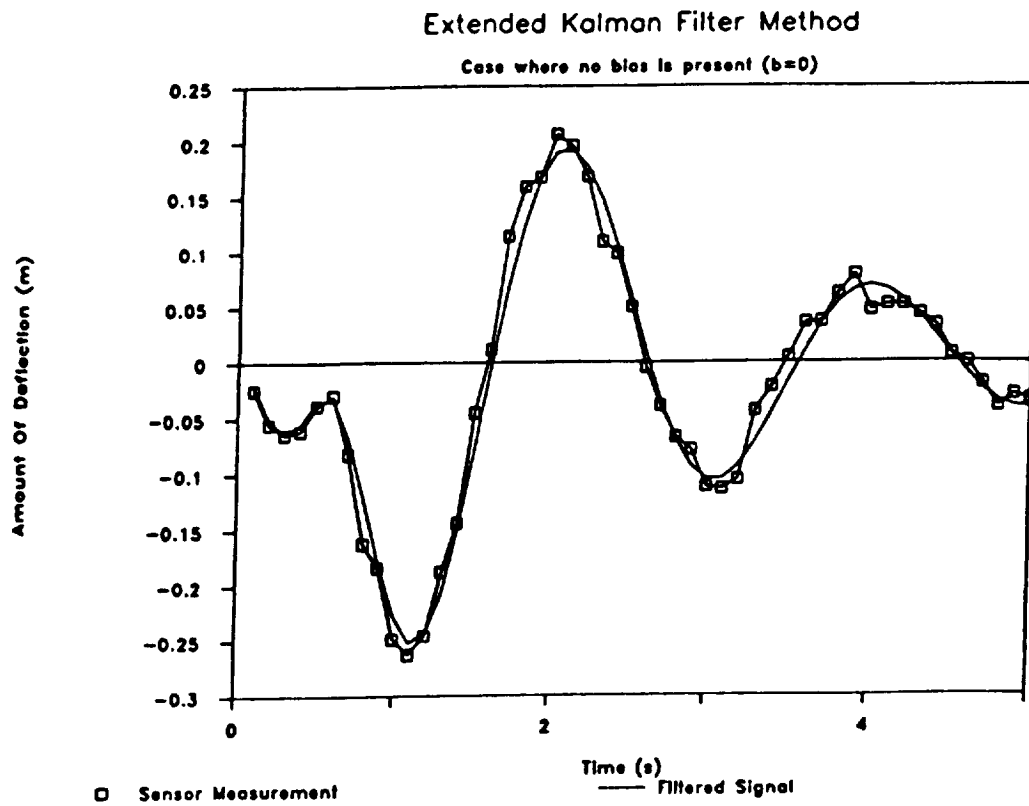


Figure 4.

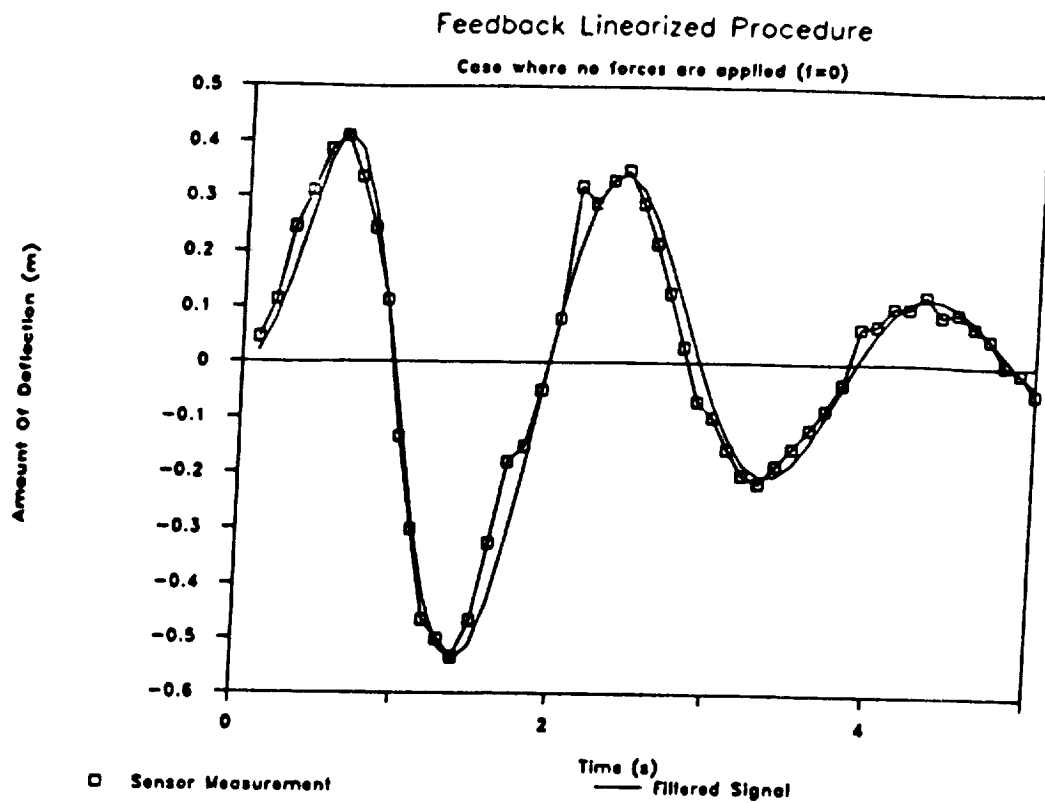


Figure 5.

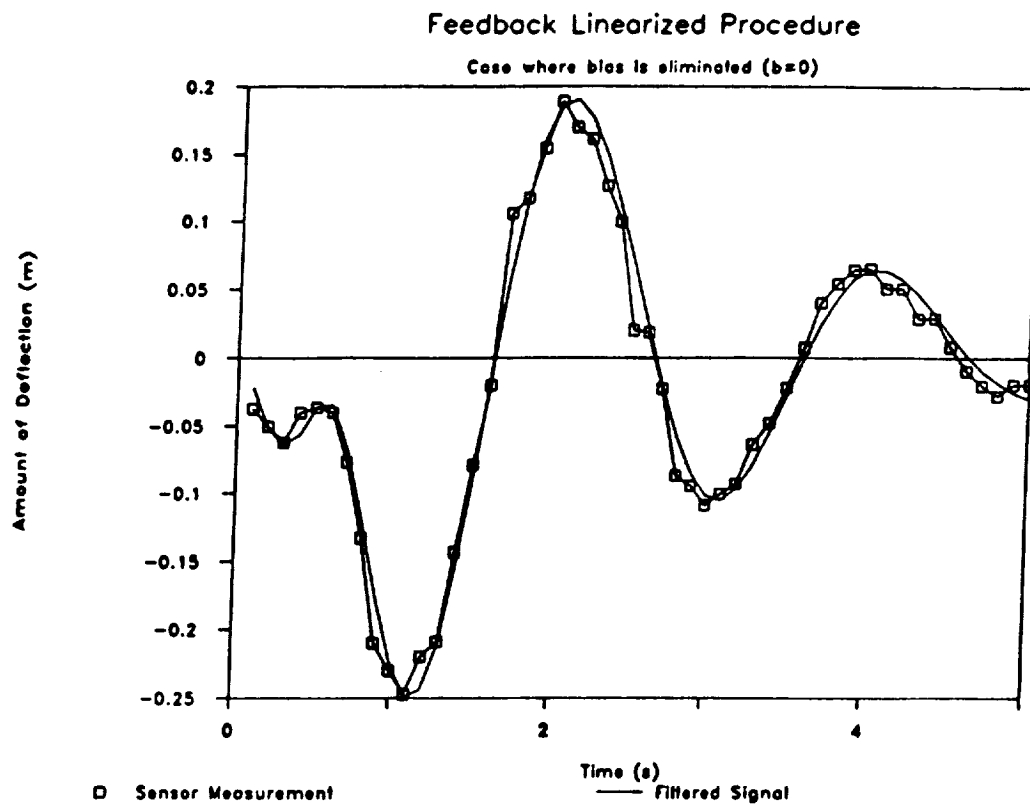
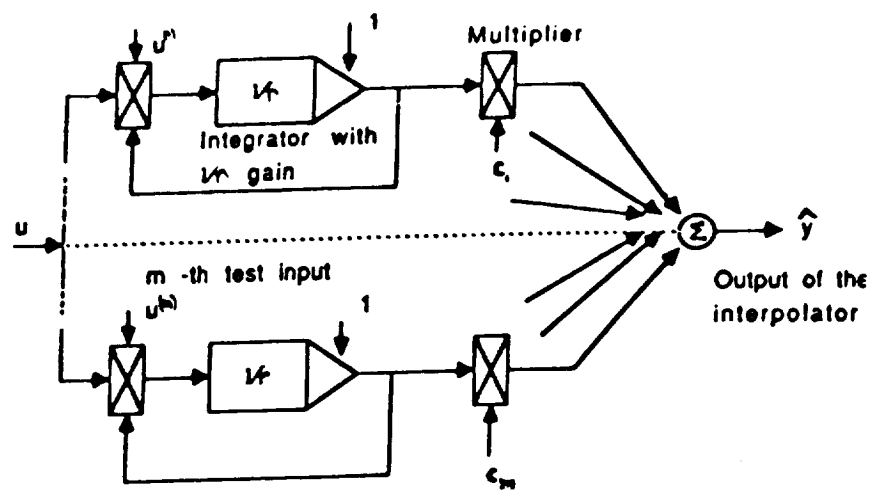


Figure 6.



Optimal Interpolator For Bilinear System

Figure 7.

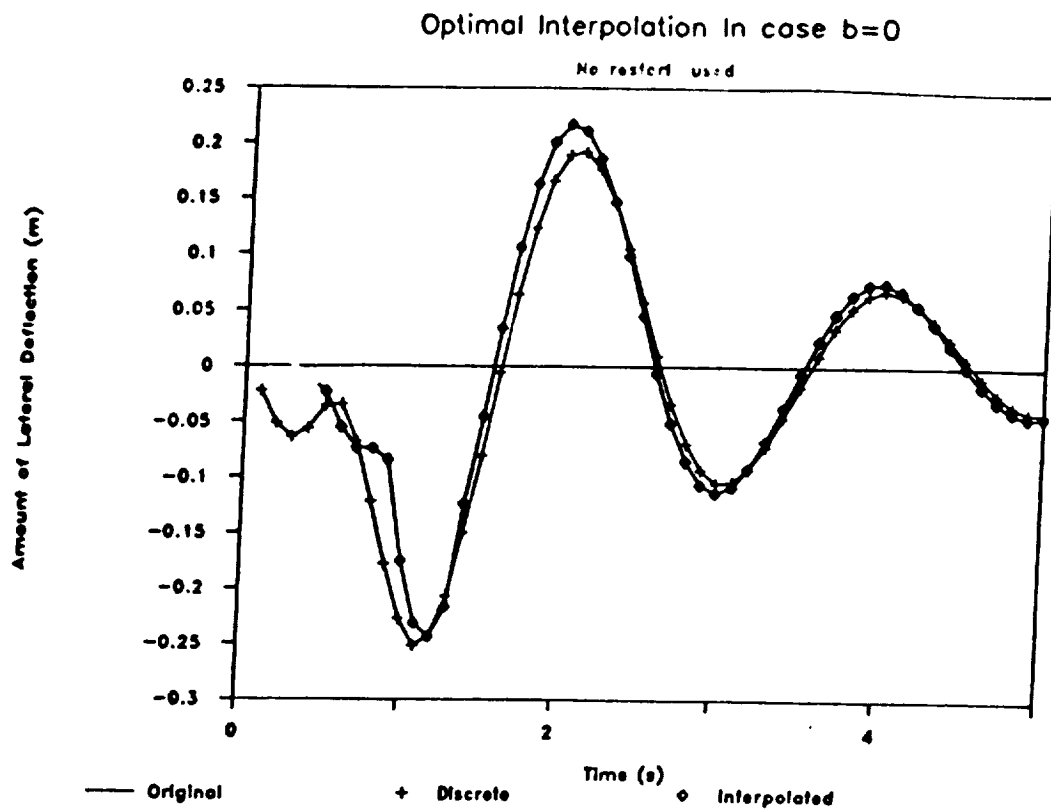


Figure 9.

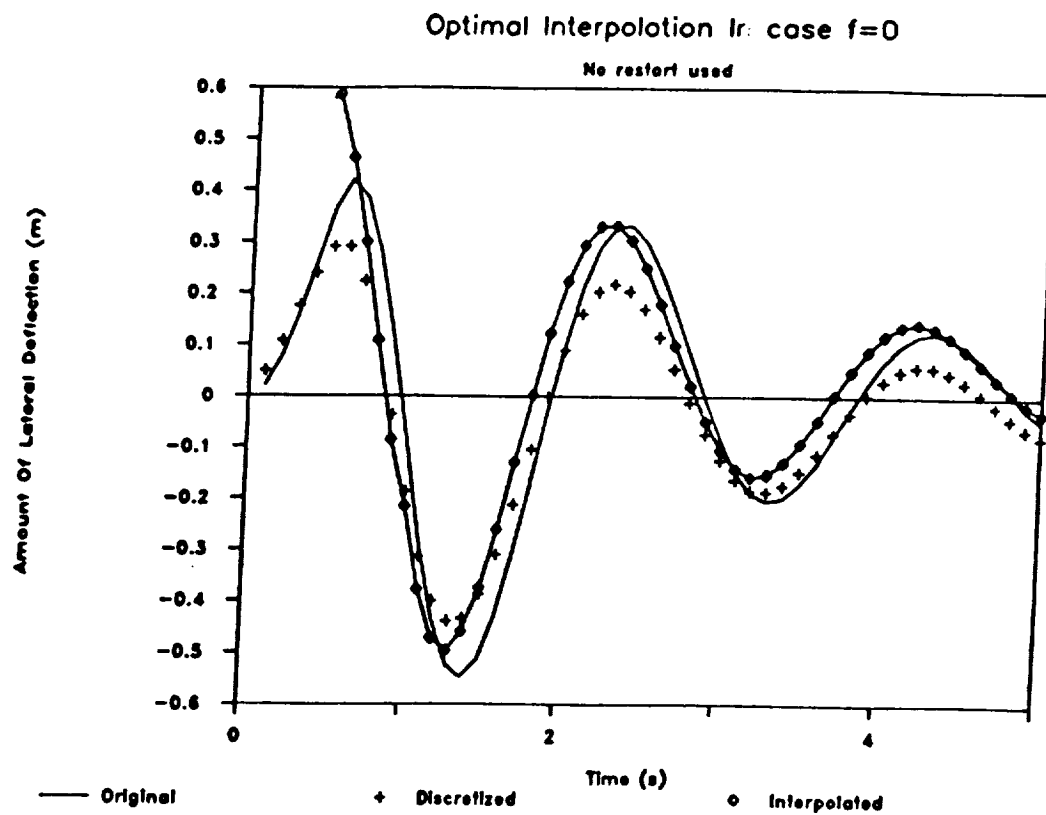


Figure 8.

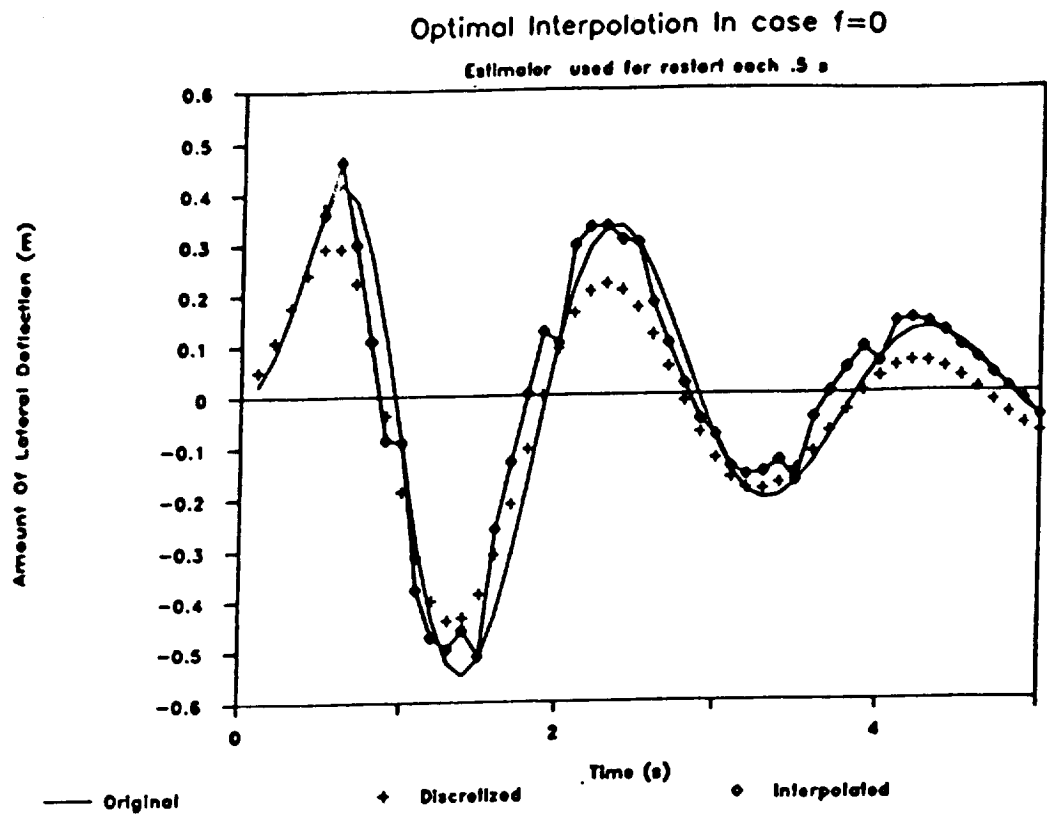


Figure 10.

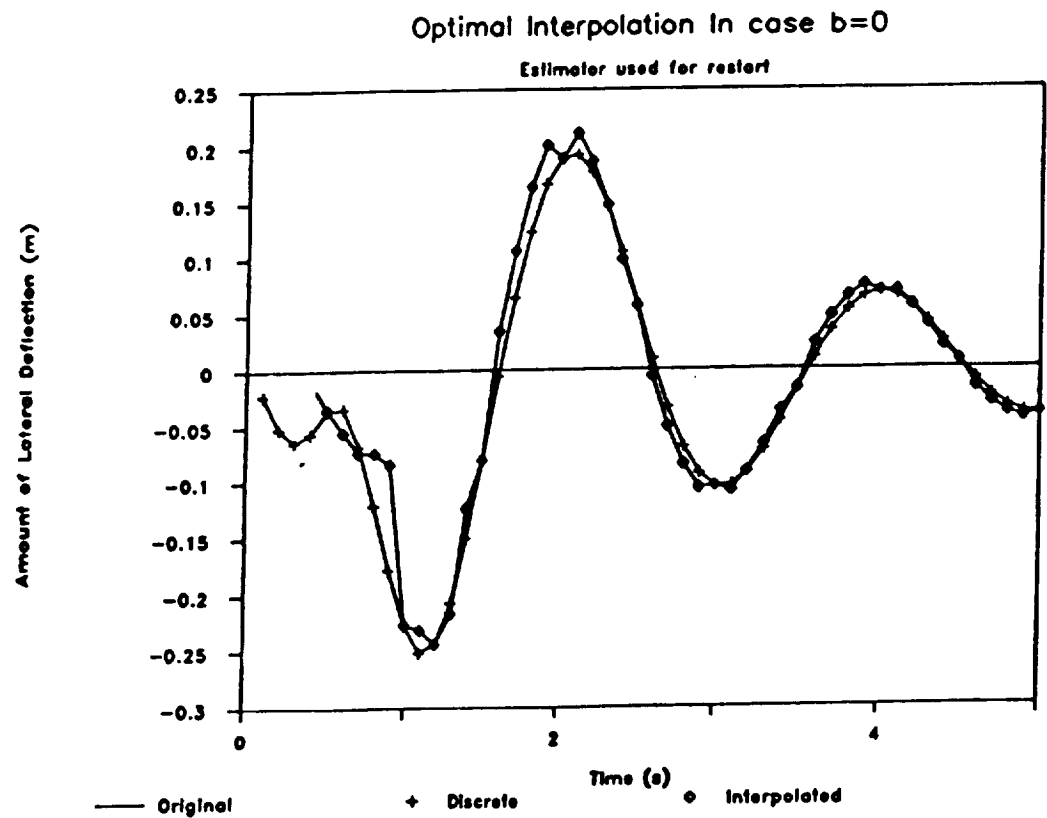


Figure 11.

